frontiers | Frontiers in Marine Science

TYPE Original Research
PUBLISHED 26 November 2024
DOI 10.3389/fmars.2024.1463564

OPEN ACCESS

EDITED BY
Julleh Rahman,
Jahangirnagar University, Bangladesh

REVIEWED BY
Rui Bao,
Ocean University of China, China
Xiting Liu,
Ocean University of China, China

*CORRESPONDENCE
Zhongshan Shen
zsshen@mail.iggcas.ac.cn
Yanping Chen
chenai0812@163.com

RECEIVED 12 July 2024
ACCEPTED 28 October 2024
PUBLISHED 26 November 2024

CITATION
Shen Z, Wang H, Chen Y, Cai Y and Yi L (2024) Sedimentary dynamics in southern Mariana Trench and its controlling factors in past 440 kyr.
Front. Mar. Sci. 11:1463564.
doi: 10.3389/fmars.2024.1463564

Sedimentary dynamics in southern Mariana Trench and its controlling factors in past 440 kyr

Zhongshan Shen[1]*, Haifeng Wang[2,3], Yanping Chen[4]*, Yun Cai[5] and Liang Yi[5]

[1]State Key Laboratory of Lithospheric and Environmental Coevolution, Institute of Geology and Geophysics, Chinese Academy of Sciences, Beijing, China, [2]Key Laboratory of Marine Mineral Resources, Ministry of Natural Resources, Guangzhou Marine Geological Survey, China Geological Survey, Guangzhou, China, [3]Southern Marine Science and Engineering Guangdong Laboratory (Guangzhou), Guangzhou, China, [4]Zhejiang Academy of Marine Sciences, Second Institute of Oceanography, Ministry of Natural Resources, Hangzhou, China, [5]State Key Laboratory of Marine Geology, Tongji University, Shanghai, China

Understanding sediment dynamics and their controlling factors is essential for Quaternary studies, yet they remain poorly documented in the Mariana Trench. In this work, we examine this basic character from a sediment core collected at a depth of 6470 m from the southern part of the Mariana Trench, documenting changes in sedimentary dynamics over the past ~440 kyr. Our primary findings are as follows: (1) The median grain size is 13.6 ± 12.0 μm, and minimal changes in clay (30.9 ± 9.4%) and silt (56.6 ± 4.0%) contents, indicating a low-dynamic depositional environment; (2) Three grain-size components were identified, characterized by modal changes of ~4/60 μm, ~20 μm, and >100 μm. By comparing these results with various environmental proxies, including glacial-interglacial alternations, eolian input, and bottom-water intensity, we suggest that marine productivity has a dominant influence on deep-sea sediment dynamics, though post-depositional processes also contribute. Additionally, topographical conditions and sea-water chemistry appear to be related to the presence of coarse particles, possibly through coarse transport and micro-nodule development. Overall, grain-size parameters provide a valuable investigative tool for understanding the various influences on sediment dynamics in this region.

KEYWORDS

sediment grain size, Mariana Trench, factor analysis, deep-sea dynamics, Western Pacific

1 Introduction

The Mariana Trench, the deepest part of the Earth's surface, reaches a maximum depth of ~11,000 m at the Challenger Deep, likely due to minimal sediment infill (Fryer et al., 2003). It lies along the boundary between the eastern Philippine Sea plate and the subducting Pacific plate (Figure 1). This region represents a non-accretionary convergent plate margin, where the basement of the overriding plate is in direct contact with the subducting plate at the trench axis (Hussong and Uyeda, 1981), with subduction beginning prior to ~50 Ma (Ranken et al., 1984; Jurdy, 1979).

Technological advances in deep-ocean exploration over the past decade have drawn significant attention to the Mariana Trench, revealing the uniqueness of its hadal environment. Research into hadal water mixing (Kawagucci et al., 2018; Maruyama et al., 2013; van Haren et al., 2017) and hadal ecosystem (Hiraoka et al., 2019; Nunoura et al., 2015; Peoples et al., 2018; Wang et al., 2019) has highlighted two important factors affecting depositional processes in the trench: eroded and windblown particles (Jiang et al., 2019; Wang et al., 2016). Moreover, an antiphase relationship between bottom-water intensity in the trench and the eastern Pacific has been identified, potentially due to the redistribution of Antarctic bottom water (AABW) into the North Pacific (Yi, 2023).

However, there is still a lack of verification of various proxies to infer the paleoenvironmental history of this region. While sediment grain size is broadly used in environmental studies, it remains unclear which factors predominantly control this basic characteristic in the trench. To better understand the paleoenvironment of the surficial sediments in this abyssal environment, we conducted a detail study of sediment grain size on a gravity core collected from the south of the Mariana Trench (Figure 1). By integrating magnetostratigraphy with authigenic beryllium isotope ($^{10}Be/^{9}Be$) analyses, a reliable age-depth model was established, and based on this geochronological framework, grain-size properties and its controlling factors were discussed on glacial-interglacial timescales in this work.

2 Methodology

2.1 The studied core

Core JL7KGC-11b (J11b; 142.34° E, 10.95° N, 6470 m water depth) was collected using a gravity piston by the R/V HAI YANG LIU HAO, Guangzhou Marine Geological Survey in June 2012, from the southern part of the Mariana Trench. The core is 67 cm in length and 7 cm in diameter, composed of light-yellow (10YR 7/8) to brown (10YR 3/3) muds (Figure 2A).

In order to establish an age-depth model for core J11b, sediment samples were firstly subjected to stepwise alternating field (AF) demagnetization up to a peak field of 90 mT, using a three-axis cryogenic magnetometer (2G Enterprise Model 755, USA) installed in a magnetically shielded room at the State Key Laboratory of Marine Geology, Tongji University. As a result, no reversal of magnetic inclination was observed in measurements. As an alternative geochronological test, $^{10}Be/^{9}Be$ ratios were employed to constrain the duration of the core, yielding an age of 405 ± 6 kyr. Together with Ba/Al ratio changes and correlating with the stacked benthic $\delta^{18}O$ record (LR04) (Lisiecki and Raymo, 2005), the geochronology of core J11b was finally established (Figure 2). Subsequently, sedimentation rates of 0.7 ± 0.2 mm/kyr for the upper part and 2.2 ± 0.4 mm/kyr for the lower part were established. All geochronological data have been previously reported in Yi (2023) and are used here to assist sediment grain-size analysis.

2.2 Grain-size measurements

A total of 122 sediment samples were collected at 5 mm intervals from core J11b for grain-size analysis. Samples were dispersed using sodium hexametaphosphate [$(NaPO_3)_6$] and subjected to ultrasonic vibrator for 6 h. Grain-size distributions were measured with a Malvern Mastersizer 2000 laser-particle size

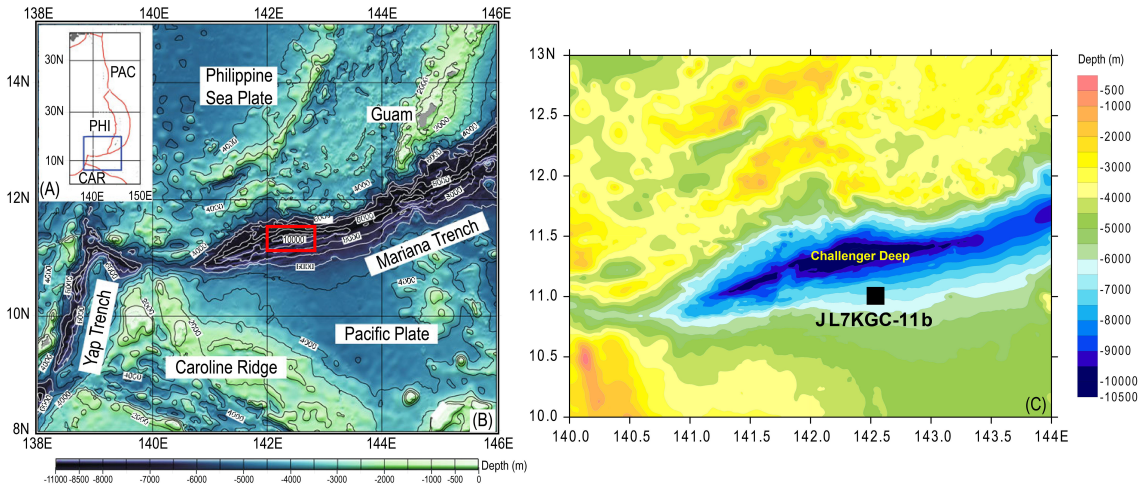

FIGURE 1
Schematic map of the Mariana Trench region as well as the location of core JL7KGC-11b. **(A)** Tectonic setting of the study area. PAC, Pacific plate; PHI, Philippine plate; CAR, Caroline Ridge. The red rectangle labels the location of the Challenger Deep. **(B)** Location of the Mariana Trench. **(C)** Location of the studied core. The bathymetric data of the Mariana Trench was downloaded from http://ccom.unh.edu/theme/law-sea/mariana-trench-pacific-ocean/.

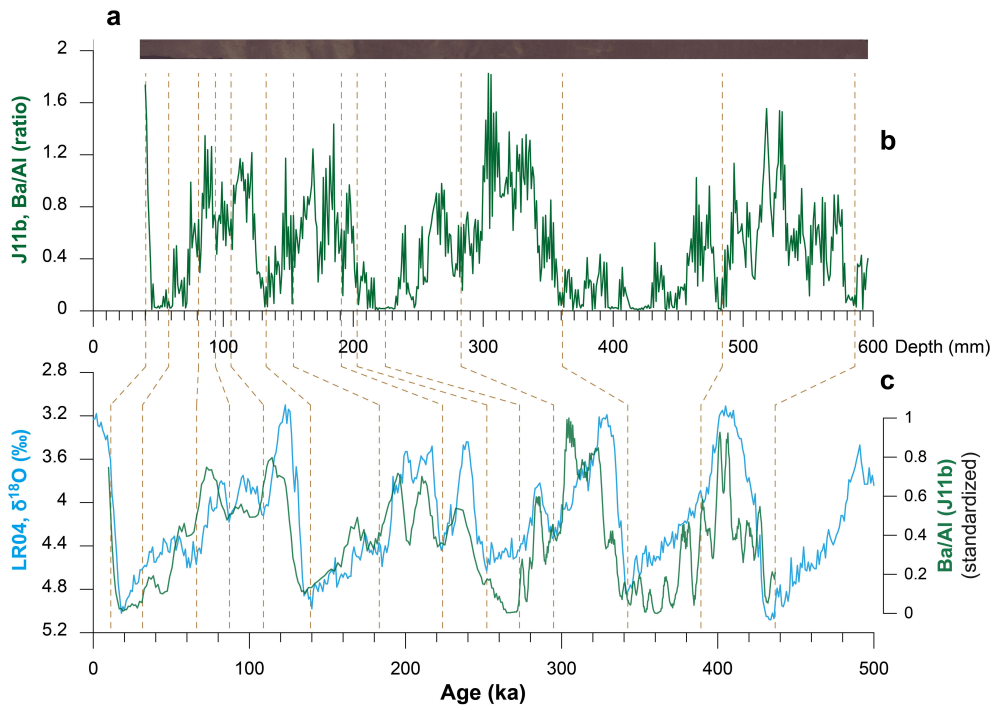

FIGURE 2
The age-depth model of core J11b. **(A)** The core photo. **(B)** Ba/Al changes of core J11b for tuning. **(C)** Benthic $\delta^{18}O$ stack LR04 (Lisiecki and Raymo, 2005) versus the tuned Ba/Al record of core J11b (11-point moving average). This tuning process was preliminary constrained by ^{10}Be dating (405 ± 6 kyr), and all of these data was reported in Yi (2023).

analyzer at Second Institute of Oceanography, Ministry of Natural Resources of China. One hundred grain size classes between 0.3 and 300 μm were analyzed using mathematical methods, including the varimax-rotated principal component analysis (VPCA), environmentally-sensitive components, and lognormal-based unmixing. The common signal of deep-sea sedimentary dynamics was extracted for paleoenvironmental inferences, following the established procedures (e.g., Boulay et al., 2003; Paterson and Heslop, 2015; Chen et al., 2020, 2021).

2.3 Lognormal-based unmixing

Grain-size spectra of sediment are often polymodal, and can be estimated by superposition of multiple unimodal components, following a particular theoretical distribution. In this study, we applied a lognormal function to the grain-size spectra. The polymodal distribution can be expressed as:

$$f = p_1 f_1 + p_2 f_2 + \ldots (1 - p_1 - p_{2-} \ldots p_{n-1}) f_n \quad (1)$$

where f_i represents the function for component i where $i = 1$ to n components, and p_i is the component's percentage in the bulk sample. Within each spectrum, there are $n-1$ coefficients, p_i, that need to be estimated due to closure. The lognormal function has the following form:

$$f(\chi, \quad \alpha, \beta) = \frac{\alpha}{\beta^{\alpha}} \chi^{\alpha-1} e^{-(\frac{\chi}{\beta})^{\alpha}} \quad (2)$$

where x represents the grain size in μm, the coefficient α determines the distribution's shape, and β controls the position of the central tendency of the curve - here, the mean grain-size curve.

Because grain-size distribution of all samples consists two components, the function formula for partitioning can be expressed by the following equation:

$$f(\chi, \alpha_1, \beta_1, p_1, \alpha_2, \beta_2) = p_1 \frac{\alpha_1}{\beta^{\alpha_1}} \chi^{\alpha_1 - 1} e^{-(\frac{\chi}{\beta_1})^{\alpha_1}} + (1 - p_1) \frac{\alpha_2}{\beta_2^{\alpha_2}} \chi^{\alpha_2 - 1} e^{-(\frac{\chi}{\beta_2})^{\alpha_2}} \quad (3)$$

The values α_1 and β_1 are parameters of the distribution function of the fine-grained component, α_2 and β_2 represent the coarse-grained component. The percentages of each component in a sub-population are given by p_1 and $(1\text{-}p_1)$, respectively. Using the measured grain-size data in one hundred grain-size classes (x), the parameters can be estimated by General Least Squares Fitting.

3 Results

3.1 Grain-size properties

The median grain size (M) throughout the studied interval of core J11b is 13.6 ± 12.0 μm, suggesting a low-dynamic depositional environment that has remained relatively stable over the past ~440 kyr (Figure 3A). Clay (< 4 μm) and silt (4~63 μm) contents showed minimal variation, with average values of 30.9 ± 9.4% and 56.6 ±

4.0%, respectively. However, sand particles (> 63 μm) exhibited greater variability, with an average value of 12.5 ± 9.2%. Similar variability can be also observed in C values (207.7 ± 122.6 μm), which represents the one percentile of grain size distribution. For the coarsest component (typically >300 μm), they are observed only in several samples, which could be micro authigenic nodules occurring in slowly accumulating marine low sediments (Wang et al., 2016), or biogenic silica debris (Lai et al., 2023). These coarse particles seem independent to other grain-size components, and consistent with sediments from surrounding regions (Yi et al., 2020, 2021).

To further characterize the sedimentary dynamics, we analyzed two parameters: C value, representing the most hydrodynamically active component, and M, the median diameter, indicating the mean hydrodynamic energy. In the C-M diagram, in which valuable insights into sediment transport and hydrodynamic intensity can be revealed (Passega, 1957, 1964), it is observed that these two parameters are generally coupled (Figure 4B). However, when C values exceed 300 μm, the most dynamic sedimentary process appears uncoupled from the dominant sedimentary components, suggesting distinct dynamics.

The grain-size distributions are bimodal, with modal sizes of ~4 μm and ~60 μm (Figure 3). Minor differences in grain-size distributions among samples indicate a stable sedimentary environment throughout the studied period. Environmentally sensitive grain-size components are useful for characterizing specific sedimentary processes and/or dynamics (Boulay et al., 2003), and they have been used in various paleoenvironmental studies (e.g., Hu et al., 2021; Sun et al., 2003). Following the method of Boulay et al. (2003), two environmentally-sensitive components were determined (Figure 3C): CC-1 and CC-2, peaking at 2.8-4.0 μm and 55.3-83.6 μm, respectively.

Polymodal grain-size spectra can be mathematically partitioned (Ashley, 1978), enabling the separation of orthogonal modes (independent grain-size components/factors) to identify potential changes in input functions and/or sedimentary dynamics (e.g., Chen et al., 2020, 2021; Yi et al., 2012a). Using lognormal-based unmixing (Paterson and Heslop, 2015), we identified two primary components (Figure 4C): EM-1 and EM-2, with modal sizes of 4.3 μm and 48.1 μm, respectively. VPCA can be also used to identify the processes controlling sediment grain-size changes and to extract paleoenvironmental signals (e.g., Hu et al., 2021; Yi, et al., 2012b). As a result, four components (VF1-VF4) account for 98.6% of the variance (Figure 4D).

Combining all the grain-size results, it is inferred that for environmentally-sensitive components and lognormal-based

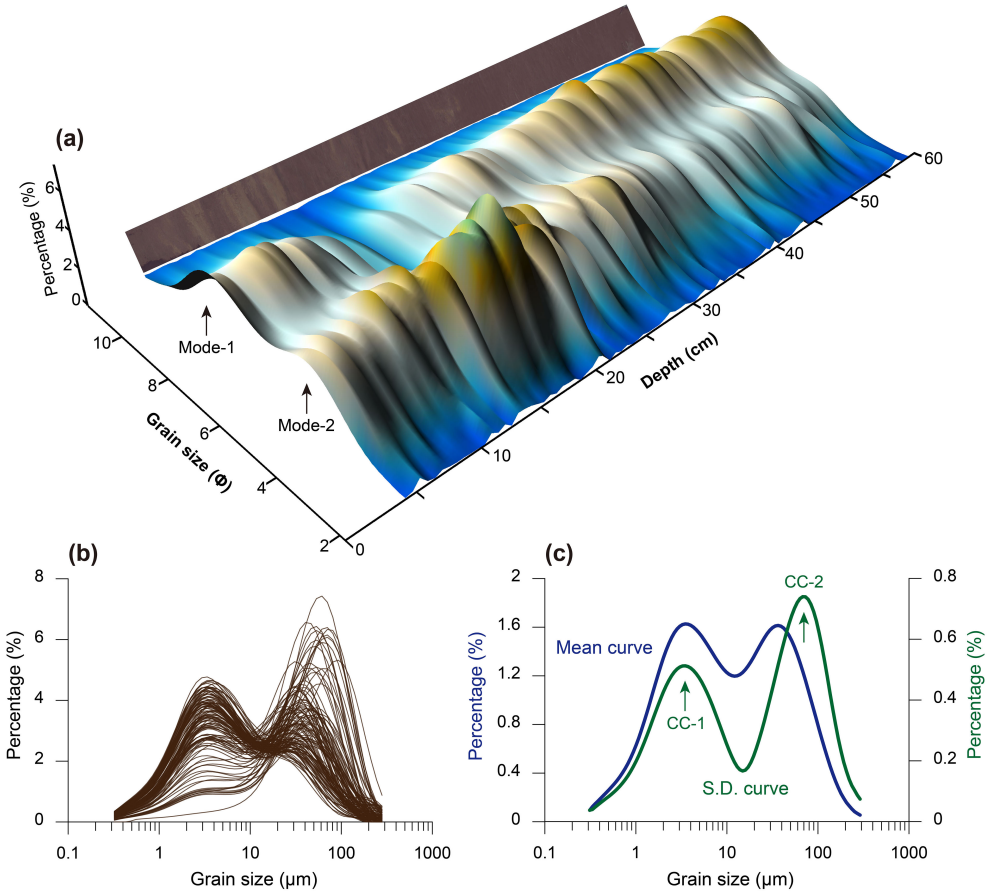

FIGURE 3
Spectral profile of sediment grain size of core J11b **(A)** with probability density function **(B)** and the results of environmentally-sensitive components (CC-1 and CC-2) **(C)**. Mean, the average grain-size curve of all samples; S.D., the standard deviation for all samples.

unmixing (Figures 3, 4), two grain-size components are similarly identified and negatively correlated with each other, suggesting a single major factor dominating sedimentary dynamics. However, for VPCA results, four extracted components may infer a more complex process, which highlights the potential of the VPCA method in analyzing grain-size data in this critical region. In details, components VF1 and VF2 are closely related to changes in CC-1 and EM-1, and CC-2 and EM-2, respectively. Components VF3 and VF4 highlight more complex processes, indicating additional sedimentary factors influencing grain-size distribution.

3.2 Changes in grain-size parameters

Constrained by the refined age-depth model, variabilities in each grain-size parameter can be revealed. As shown in Figure 5, four key grain-size parameters, including median size (M), and clay, silt and sand contents, are well correlated with each other in the past ~440 kyr. For example, clay and silt contents exhibit negative correlations with median size (M) and sand content, respectively. During 150-300 ka, all grain-size parameters display a significant shift. This variation is similarly reflected in the derived grain-size components, including EM1, EM2, VF1, and VF2 (Figure 6), supporting the inference that a single major factor dominating sedimentary dynamics in the study area during the depositional interval.

Interestingly, for the most hydrodynamic sedimentary component, the C value exhibits distinct variability. Although not as pronounced as other parameters, it generally aligns with glacial-interglacial alternations (Figure 5B). This pattern is also observed in the VF4 record (Figure 6D). Specifically, during interglacial intervals, such as since <20 ka, 70-130 ka, 190-240 ka, 300-340 ka, and 370-420 ka, C values were significantly lower compared to glacial periods, suggesting relatively low sedimentary dynamics in the study area during these intervals. The VF3 component, according to the VPCA eigenvalues (Figure 4D), appears to reflect different variabilities compared to VF1, VF2, and VF4. This observation implies that, although the dominant processes remained consistent and characterized by low dynamics over the past ~440 kyr, the dispersion between C and M values suggests the influence of high-dynamic processes in core J11b, which may be responsible for the dominance of coarse particles in the sediments on glacial-interglacial timescales.

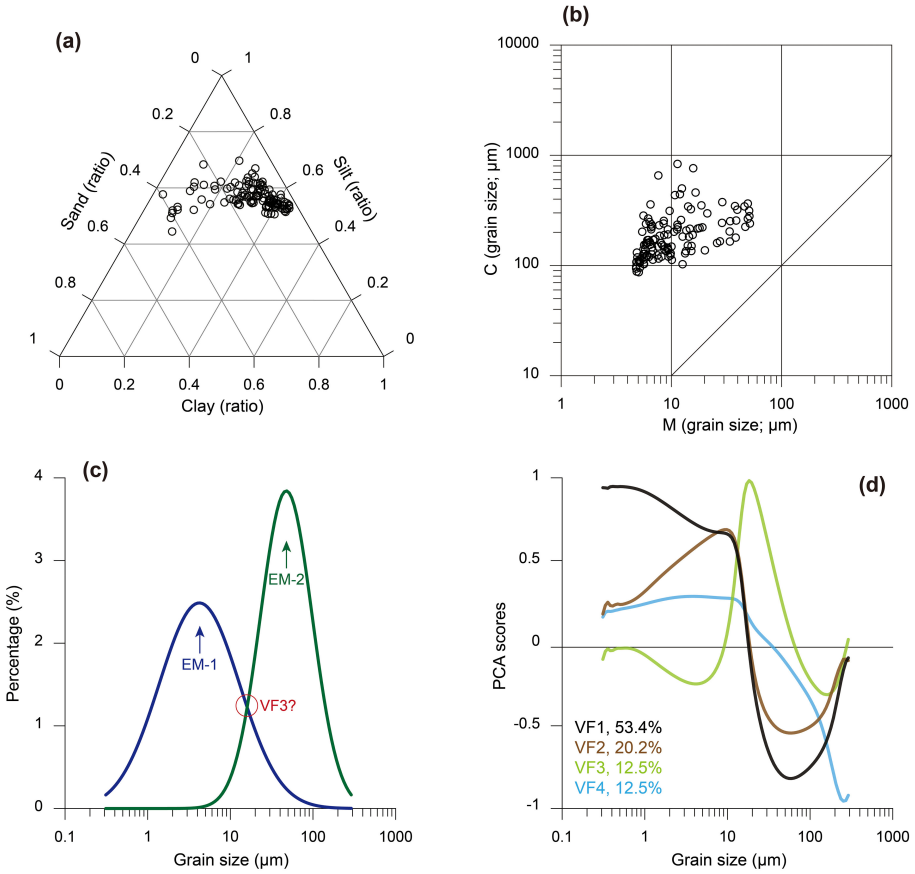

FIGURE 4
Characteristics of sediment grain size of core J11b. **(A)** Ternary diagrams; **(B)** C-M diagrams; **(C)** Unmixing results. EM-1 and EM-2 are the two characterized grain-size components through mathematical partitioning of sediment grain-size spectrum; **(D)** Principal component analysis, VF1-VF4 are the four components by VPCA.

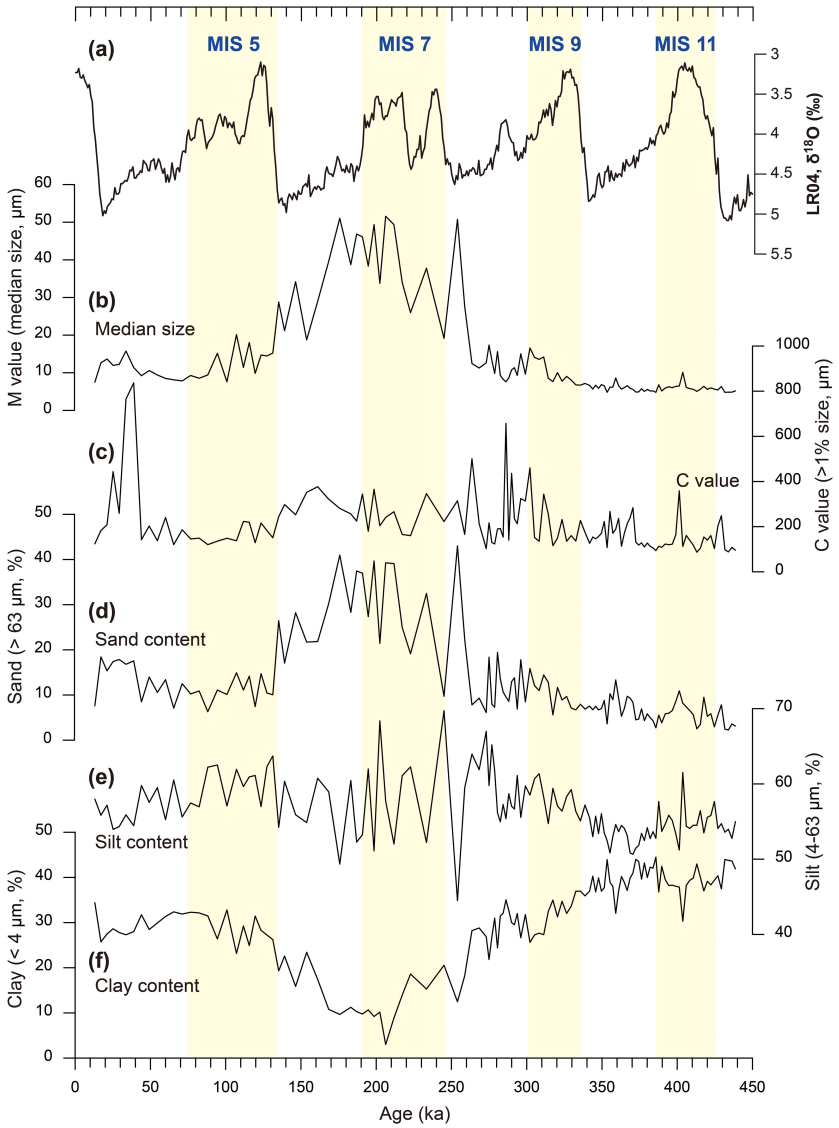

FIGURE 5
Comparison between the LR04 **(A)** and grain-size variabilities of core J11b **(B–F)**.

4 Discussion

4.1 Productivity influence on low-dynamics processes

By analyzing the sedimentary dynamics in the study area, several influencing factors were identified, allowing for the reconstruction of sedimentary history over the past 440 kyr. Considering the grain-size pretreatment listed in the method part (section 2.2), biogenic particles from the upper ocean are firstly testified, such as silica/carbonate debris and organic matters that were not removed before grain-size measurement.

As shown (Figure 7), elemental changes, including Si, K, and Ca, show strong correlations with grain-size variations in core J11b, while this agreement is less evident when compared to the benthic $\delta^{18}O$ stack LR04, which is a proxy for Northern Hemisphere glaciation (Lisiecki and Raymo, 2005).

Calcium content in deep-sea sediments is generally linked to biogenic changes (Murray and Leinen, 1993; Yi et al., 2021), and is often used for geochronological tuning (Bickert and Henrich, 2011; Farrell and Prell, 1989; Jakob et al., 2018). However, in some deep-sea sites below the CCD (typically >4,000 m in the Pacific), such as core I8 from the west Philippine Sea (Xu et al., 2022), core GC18 near the Marshall seamount (Wang et al., 2023), and core J01A from the Mariana Trench (Yi et al., 2020), the relationship between calcium changes and the LR04 record is not as clear. The great water depth and the locality-specific influences (Anderson et al., 2008; Qin et al., 2018) could be the potential factors for this discrepancy

10.3389/fmars.2024.1463564

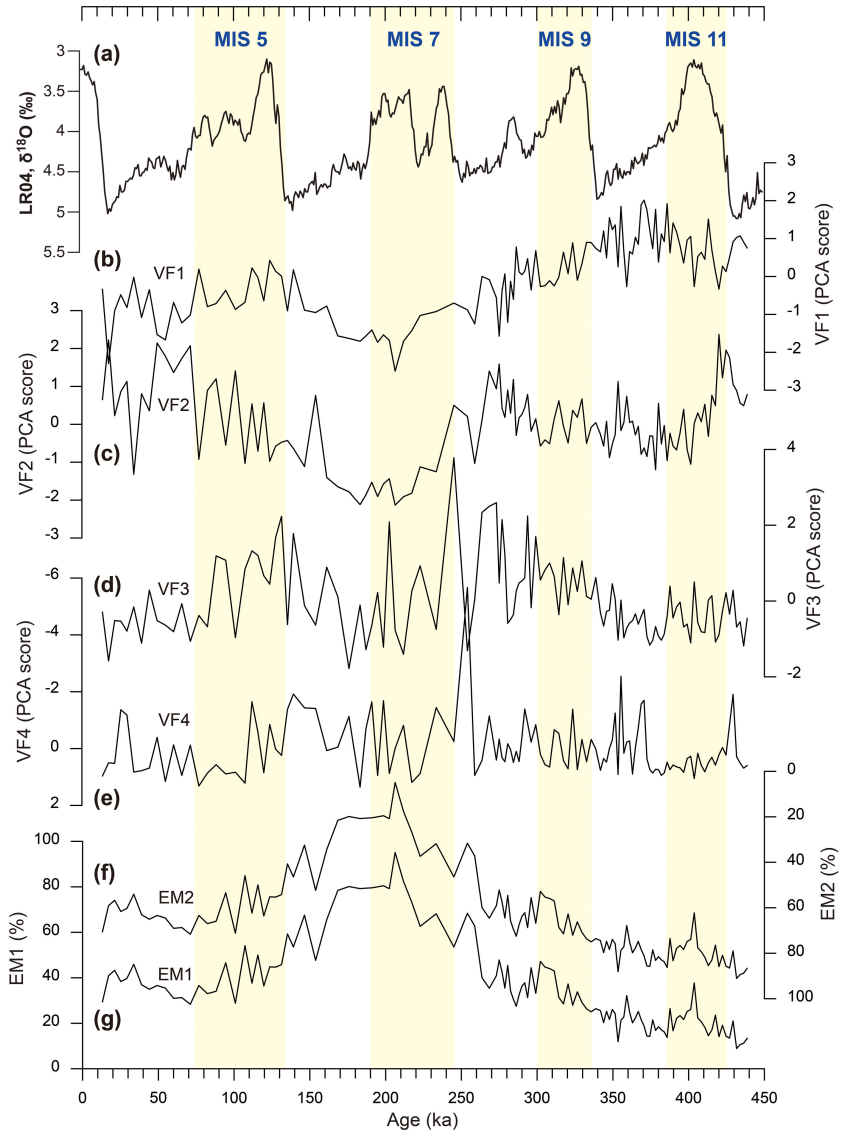

FIGURE 6
Comparison between the LR04 **(A)** and the derived parameters of core J11b **(B–G)**.

between sedimentary Ca and the LR04, likely involving an interaction between marine productivities and post-deposition processes (Xu et al., 2022; Wang et al., 2023). In this case, the negative relationship between Ca content and M value observed in core J11b might suggest that when carbonate particles fell through the CCD, their sizes significantly reduced due to the dissolving processes, possibly resulting in carbonate residuals with a very fine size deposited in the sediments.

On the other hand, the proxies from core J11b shown in Figure 7 exhibit a long-term V-shaped trend from MIS 8 to MIS 5 (~300-100 ka), which correlates with the highest Si value and the light-yellow color of the sediments (Figure 2). Biogenic silica, primarily distributed around the Antarctica and the North Pacific (Moore, 2008; Shibamoto and Harada, 2010; Luo et al., 2022), is linked to regions of high nutrient concentrations and primary productivity (Lisitzin, 1966; Broecker and Peng, 1982; Martin, 1990). Considering the relatively larger size of biogenic silica observed in the deep-sea sediments (Lai et al., 2023), the positive relationship between Si content and M value may illustrate that the increased production of biogenic silica could significantly enlarge the sediment grain size.

Hence, it is summarized that the consistency between elements Ca, K, Si, and sediment grain-size parameters such as M values, EM1, and VF1 suggests that marine productivity may have influenced sediment dynamics in deep-sea environments, while the contributions of post-depositional processes are worthy of investigation in future to further clarify the influences from productivity changes.

4.2 Influences from eolian dust and bottom water

Eroded and windblown particles are two important factors affecting depositional processes in the trench (Jiang et al., 2019;

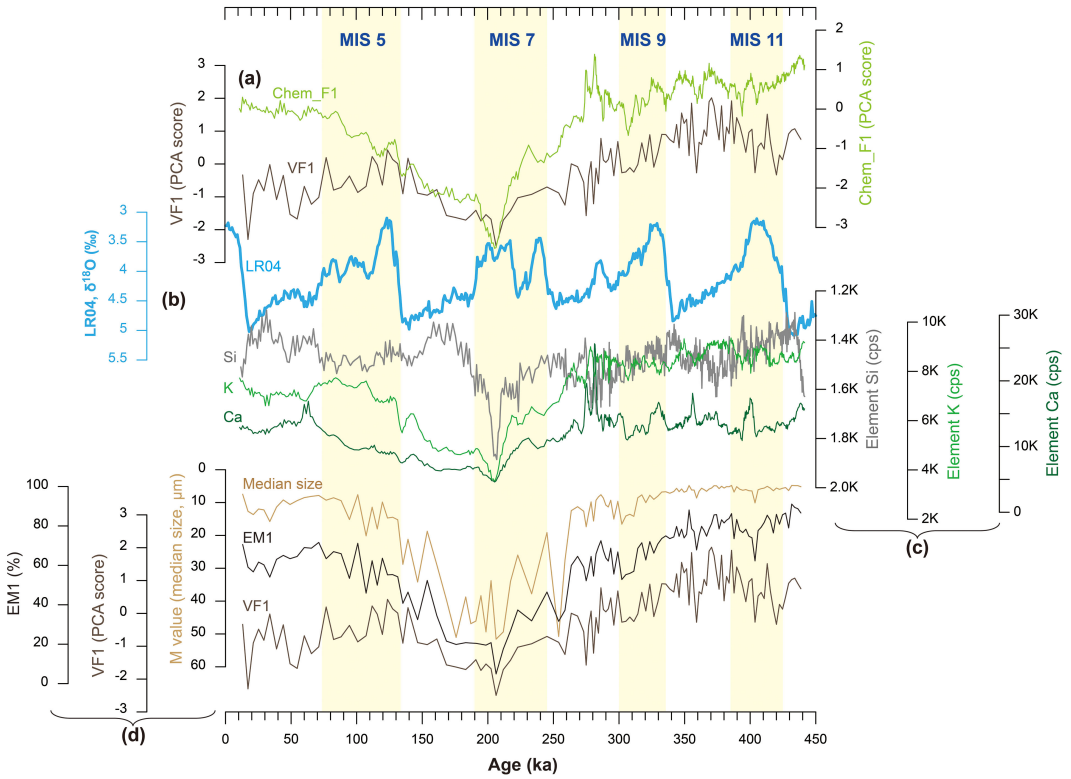

FIGURE 7
Comparisons between various productivity-related proxies. **(A)** The leading components of grain-size and geochemical results; **(B)** Benthic $\delta^{18}O$ stack LR04 (Lisiecki and Raymo, 2005); **(C)** Elemental changes from XRF scanning of core J11b (Yi, 2023); **(D)** Grain-size parameters of core J11b derived from this study. See notes in Figures 3, 4.

Wang et al., 2016), and bottom-water currents can be reconstructed by grain-size analyses (Hall et al., 2001; Yi et al., 2022; Lamy et al., 2024). Eolian particles, transported from the Asian interior (Jiang et al., 2019; Wang et al., 2016; Xiao et al., 2020), can account for up to 75% of non-biogenic components in deep-sea sediments (Windom, 1969). AABW flows across the North Pacific and serves as the primary source of dissolved oxygen in the trench (Xiao et al., 2020), making it critical to reconstruct the influences of AABW on western Pacific sedimentation using oxygen-sensitive elements (Yi, 2023).

In previous studies, a pattern of increased eolian dust during glacial periods and decreased input during interglacial periods was observed in the North Pacific (e.g., Zhang et al., 2018). This pattern is similarly reflected in variabilities of C values and VF4 record of core J11b (Figure 8). Specifically, when eolian dust decreased during interglacial periods, the C values were low, while the VF4 record was high (Figure 8B), indicating reduced sedimentary dynamics during interglacial intervals in the study site.

However, both the C values and the VF4 record are characterized by coarse particles, typically > 200 μm. These coarse particles are unlikely to be transported by winter monsoon or the westerlies, and may originate from proximal sources, such as materials dropping from the upper slope of the trench. Additionally, elemental ratios such as Ba/Al exhibit similar variability between glacial and interglacial alternations (Figure 8B). This ratio was used to refine the age-depth model of the studied core (Yi, 2023), though marine productivity may show different relationships with glacial periods as aforementioned. For example, carbonate preservation in many Pacific sites is higher during glacial intervals ('Pacific style'), a phenomenon linked to seawater chemistry changes (Anderson et al., 2008) and likely initiated from ~1.1 Ma (Sexton and Barker, 2012), while in Atlantic sites ('Atlantic style'), carbonate content tends to be higher during interglacial intervals (Qin et al., 2018; Sexton and Barker, 2012; and references therein). These complex responses of marine productivity suggest that these coarse particles in the study area are not directly related to regional productivity. Instead, considering micro-nodules tending to form in an oxygenation environment (Wang et al., 2016), sea-water chemistry in the trench related to bottom-water evolution likely influenced the development of micro-nodules in the sediments, and topographic conditions might induce the transport of coarse particles from the upper part of the trench.

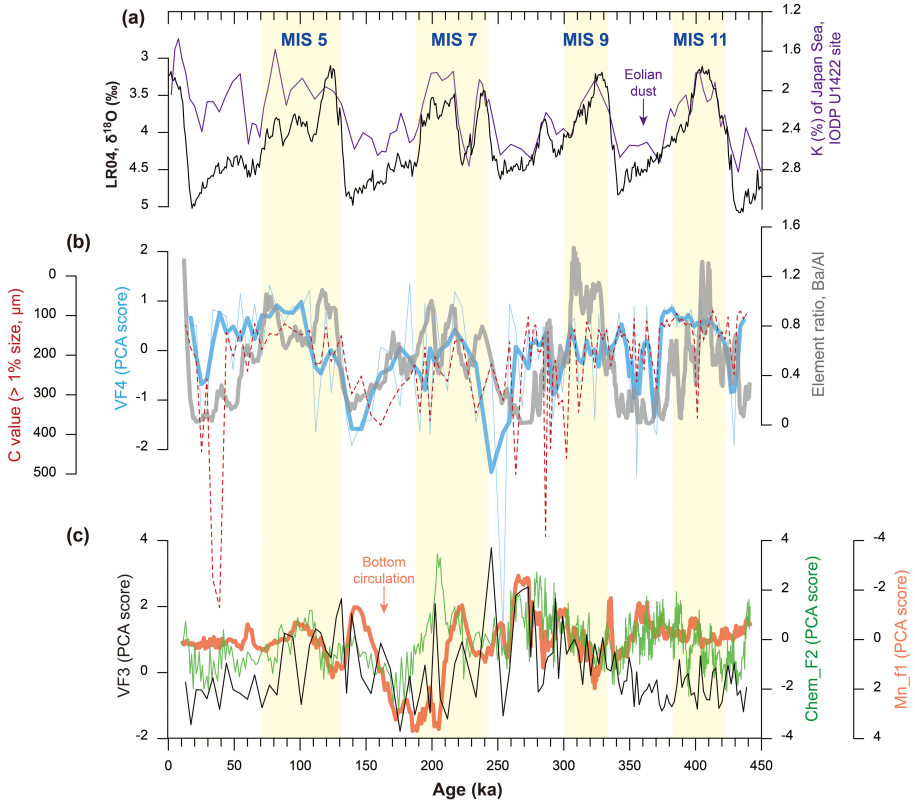

FIGURE 8
Comparisons between various environmental proxies. **(A)** Benthic $\delta^{18}O$ stack LR04 (Lisiecki and Raymo, 2005), *versus* the K content of IODP Site U1422 in the Japan Sea (Zhang et al., 2018), indicating eolian dusts to the North Pacific; **(B)** C values and VF4 record of core J11b (this study), versus elemental ratios of Ba/Al for age tuning of core J11b (Yi, 2023); **(C)** Comparison for proxies of bottom water intensity, including VF3, and two geochemical PCA components. Chem_F2 was derived elemental contents of core J11b (recalculating in this study), and Mn_f1 was from elemental ratios of three cores (Yi, 2023). See notes in Figures 3, 4.

Additionally, an agreement between the VF3 record and oxygen-sensitive proxies of bottom-water evolution in core J11b was observed in the comparisons (Figure 8B). These oxygen-sensitive proxies have been employed to make regional inferences regarding bottom-water evolution over the past 1.2 Myr (Yi, 2023). The VF3 component likely represents the shifting position of intersection between two major grain-size groups (Figure 4C), suggesting that oceanic circulation in the trench affects the inflection points between these two dynamic groups, rather than altering their modal sizes.

5 Conclusions

By studying core J11b in terms of sediment grain size and geochronology, we have documented significant changes in the sedimentary dynamics of the southern Mariana Trench over the past ~440 kyr. Our findings indicate that the median value of sediment grain size is 13.6 ± 12.0 μm, and clay and silt particles exhibit minimal variation, with average values of 30.9 ± 9.4%, and 56.6 ± 4.0%, respectively. The variance in sand particles, however, was relatively large, with an average of 12.5 ± 9.2%. These observations suggest a low-dynamic sedimentary process that has remained largely stable over the past 440 kyr, with a single major factor dominating sedimentary dynamics.

Through comparisons of these results with various environmental proxies, the dominant influence of marine productivities on deep-sea dynamic processes was confirmed, although post-depositional processes also played a role. Topographical conditions and seawater chemistry were found to influence the transport of coarse particles, as well as the development of micro-nodules in the sediments.

Therefore, we concluded that grain-size parameters are a useful tool for detecting sedimentary properties in the trench. These parameters reflect a combination of influences, including marine productivity, sediment sources, topography, and bottom-water intensify. Future paleoenvironmental inferences should incorporate cross-validation with other evidence to improve accuracy and reliability.

Data availability statement

The datasets presented in this study can be found in online repositories. The names of the repository/repositories and accession number(s) can be found in the article/supplementary material.

Author contributions

ZS: Writing – review & editing, Writing – original draft, Methodology, Funding acquisition, Formal analysis. HW: Writing – review & editing, Investigation, Data curation. YPC: Writing – review & editing, Formal analysis, Data curation. YC: Writing – review & editing, Formal analysis, Data curation. LY: Writing – review & editing, Methodology, Conceptualization.

Funding

The author(s) declare financial support was received for the research, authorship, and/or publication of this article. The work was supported by the National Natural Science Foundation of China (42304084, 41602349, 42177422), and the China Postdoctoral Science Foundation (2023M743469).

Conflict of interest

The authors declare that the research was conducted in the absence of any commercial or financial relationships that could be construed as a potential conflict of interest.

Publisher's note

All claims expressed in this article are solely those of the authors and do not necessarily represent those of their affiliated organizations, or those of the publisher, the editors and the reviewers. Any product that may be evaluated in this article, or claim that may be made by its manufacturer, is not guaranteed or endorsed by the publisher.

References

Anderson, R. F., Fleisher, M. Q., Lao, Y., and Winckler, G. (2008). Modern CaCO3 preservation in equatorial Pacific sediments in the context of late-Pleistocene glacial cycles. *Mar. Chem.* 111, 30–46. doi: 10.1016/j.marchem.2007.11.011

Ashley, G. M. (1978). Interpretation of polymodal sediments. *J. Geol.* 86, 411–421. doi: 10.1086/649710

Bickert, T., and Henrich, R. (2011). "Chapter 12 - climate records of deep-sea sediments: towards the Cenozoic ice house," in *Developments in Sedimentology*. Eds. H. HüNeke and T. Mulder (Elsevier) 63, 793–823. doi: 10.1016/B978-0-444-53000-4.00012-3

Boulay, S., Colin, C., Trentesaux, A., Pluquet, F., Bertaux, J., and Blamart, D. (2003). "Mineralogy and sedimentology of Pleistocene sediment in the South China Sea (ODP Site 1144)," in *Proceedings of the ocean drilling program, scientific results*, 184, 1–21. doi: 10.2973/odp.proc.sr.184.211.2003

Broecker, W. S., and Peng, T. H. (1982). *Tracers in the Sea* (New York: Lamont–Doherty Geological Observatory, Palisades. Observatory, Palisades, Columbia University), 690.

Chen, Y., Li, Y., Lyu, W., Xu, D., Han, X., Fu, T., et al. (2020). A 5000-year sedimentary record of east asian winter monsoon from the northern muddy area of the east China sea. *Atmosphere* 11, 1376. doi: 10.3390/atmos11121376

Chen, Y., Lyu, W., Fu, T., Li, Y., and Yi, L. (2021). Centennial impacts of the east asian summer monsoon on holocene deltaic evolution of the huanghe river, China. *Appl. Sci.* 11, 2799. doi: 10.3390/app11062799

Farrell, J. W., and Prell, W. L. (1989). Climatic change and CaCO3 preservation: an 800,000 year bathymetric reconstruction from the central equatorial Pacific Ocean. *Paleoceanography* 4, 447–466. doi: 10.1029/PA004i004p00447

Fryer, P., Becker, N., Appelgate, B., Martinez, F., Edwards, M., and Fryer, G. (2003). Why is the Challenger Deep so deep? *Earth Planet. Sc. Lett.* 211, 259–269. doi: 10.1016/S0012-821X(03)00202-4

Hall, I. R., McCave, I.N., Shackleton, N. J., Weedon, G. P., and Harris, S. E. (2001). Intensified deep pacific inflow and ventilation in pleistocene glacial times. *Nature* 412, 809–812. doi: 10.1038/35090552

Hiraoka, S., Hirai, M., Matsui, Y., Makabe, A., Minegishi, H., Tsuda, M., et al. (2019). Microbial community and geochemical analyses of trans-trench sediments for understanding the roles of hadal environments. *ISME. J.* 14, 740–756. doi: 10.1038/s41396-019-0564-z

Hu, B., Yi, L., Zhao, J., Guo, J., Ding, X., Wang, F., et al. (2021). Magnetostratigraphy of core XT06 and Quaternary sedimentary dynamics of the deep-sea deposits in the West Philippine Basin. *Mar. Geol. Quat. Geol.* 41, 61–74. doi: 10.16562/j.cnki.0256-1492.2020101301

Hussong, D. M., and Uyeda, S. (1981). *Tectonic processes and the history of the Mariana Arc: A synthesis of the results of Deep Sea Drilling Project Leg 60, Initial Reports of the Deep Sea Drilling Project* (Texas, USA: Ocean Drilling Program (ODP)). 909–929.

Jakob, K. A., Pross, J., Scholz, C., Fiebig, J., and Friedrich, O. (2018). Thermocline state change in the eastern equatorial Pacific during the late Pliocene/early Pleistocene intensification of Northern Hemisphere glaciation. *Clim. Past.* 14, 1079–1095. doi: 10.5194/cp-14-1079-2018

Jiang, Z., Sun, Z., Liu, Z., Cao, H., Geng, W., Xu, H., et al. (2019). Rare-earth element geochemistry reveals the provenance of sediments on the southwestern margin of the Challenger Deep. *J. Oceanol. Limnol.* 37, 998–1009. doi: 10.1007/s00343-019-8046-8

Jurdy, D. M. (1979). Relative plate motions and the formation of marginal basins. *J. Geophys. Res. Solid. Earth* 84, 6796–6802. doi: 10.1029/JB084iB12p06796

Kawagucci, S., Makabe, A., Kodama, T., Matsui, Y., Yoshikawa, C., Ono, E., et al. (2018). Hadal water biogeochemistry over the Izu–Ogasawara Trench observed with a full-depth CTD-CMS. *Ocean. Sci.* 14, 575–588. doi: 10.5194/os-14-575-2018

Lai, W., Liu, X., Tian, J., Wang, H., Zhang, J., Huang, J., et al. (2023). Mineralogy of sediments in the mariana trench controlled by environmental conditions of the west pacific since the last glacial maximum. *J. Asian Earth Sci.* 245, 105553. doi: 10.1016/j.jseaes.2023.105553

Lamy, F., Winckler, G., Arz, H. W., Farmer, J. R., Gottschalk, J., Lembke-Jene, L., et al. (2024). Five million years of antarctic circumpolar current strength variability. *Nature* 627, 789–796. doi: 10.1038/s41586-024-07143-3

Lisiecki, L. E., and Raymo, M. E. (2005). A Pliocene-Pleistocene stack of 57 globally distributed benthic δ18O records. *Paleoceanography* 20, (1). doi: 10.1029/2004pa001071

Lisitzin, A. P. (1966). "Basic law of distribution of recent siliceous sediments and their relation to climatic zonality," in *Geochemistry of Silica (Russian)* (Nauka, Moscow), 241–267.

Luo, M., Li, W., Geilert, S., Dale, A. W., Song, Z., and Chen, D. (2022). Active silica diagenesis in the deepest hadal trench sediments. *Geophys. Res. Lett.* 49, (14). doi: 10.1029/2022gl099365

Martin, J. H. (1990). Glacial-interglacial CO2 change: the iron hypothesis. *Paleoceanography* 5, 1–13. doi: 10.1029/PA005i001p00001

Maruyama, S., Behnia, M., Chisaki, M., Kogawa, T., Okajima, J., and Komiya, A. (2013). Large eddy simulation of the diffusion process of nutrient-rich up-welled seawater. *Front. Heat. Mass. Tran.* 4, 1–6. doi: 10.5098/hmt.v4.2.3002

Moore, T. C. Jr (2008). Chert in the Pacific: Biogenic silica and hydrothermal circulation. *Palaeogeogr. Palaeoclimatol. Palaeoecol.* 261, 87–99. doi: 10.1016/j.palaeo.2008.01.009

Murray, R. W., and Leinen, M. (1993). Chemical transport to the seafloor of the equatorial Pacific Ocean across a latitudinal transect at 135°W: Tracking sedimentary major, trace, and rare earth element fluxes at the Equator and the Intertropical Convergence Zone. *Geochim. Cosmochim. Acta* 57, 4141–4163. doi: 10.1016/0016-7037(93)90312-K

Nunoura, T., Takaki, Y., Hirai, M., Shimamura, S., Makabe, A., Koide, O., et al. (2015). Hadal biosphere: Insight into the microbial ecosystem in the deepest ocean on Earth. *Proc. Natl. Acad. Sci.* 112, E1230–E1236. doi: 10.1073/pnas.1421816112

Passega, R. (1957). Texture as characteristic of clastic deposition1. *AAPG. Bull.* 41, 1952–1984. doi: 10.1306/0bda594e-16bd-11d7-8645000102c1865d

Passega, R. (1964). Grain size representation by CM patterns as a geologic tool. *J. Sediment. Res.* 34, 830–847. doi: 10.1306/74d711a4-2b21-11d7-8648000102c1865d

Paterson, G. A., and Heslop, D. (2015). New methods for unmixing sediment grain size data. *Geochem. Geophy. Geosy.* 16, 4494–4506. doi: 10.1002/2015gc006070

Peoples, L. M., Donaldson, S., Osuntokun, O., Xia, Q., Nelson, A., Blanton, J., et al. (2018). Vertically distinct microbial communities in the Mariana and Kermadec trenches. *PloS One* 13, e0195102. doi: 10.1371/journal.pone.0195102

Qin, B., Li, T., Xiong, Z., Algeo, T. J., and Jia, Q. (2018). Deep-water carbonate ion concentrations in the western tropical pacific since the mid-pleistocene: A major perturbation during the mid-brunhes. *J. Geophys. Res. Oceans.* 123, 6876–6892. doi: 10.1029/2018JC014084

Ranken, B., Cardwell, R. K., and Karig, D. E. (1984). Kinematics of the philippine sea plate. *Tectonics* 3, 555–575. doi: 10.1029/TC003i005p00555

Sexton, P. F., and Barker, S. (2012). Onset of 'Pacific-style' deep-sea sedimentary carbonate cycles at the mid-Pleistocene transition. *Earth Planet. Sc. Lett.* 321-322, 81–94. doi: 10.1016/j.epsl.2011.12.043

Shibamoto, Y., and Harada, K. (2010). Silicon flux and distribution of biogenic silica in deep-sea sediments in the western North Pacific Ocean. *Deep-Sea. Res.* Pt I 57, 163–174. doi: 10.1016/j.dsr.2009.10.009

Sun, Y., Gao, S., and Li, J. (2003). Preliminary analysis of grain-size populations with environmentally sensitive terrigenous components in marginal sea setting. *Chin. Sci. Bull.* 48, 184–187. doi: 10.1360/03tb9038

van Haren, H., Berndt, C., and Klaucke, I. (2017). Ocean mixing in deep-sea trenches: New insights from the Challenger Deep, Mariana Trench. *Deep-Sea. Res.* Pt I 129, 1–9. doi: 10.1016/j.dsr.2017.09.003

Wang, H., Deng, X., Yi, L., Zhao, G., Li, Y., and Tu, G. (2023). Dominant eccentricity cycles in paleoenvironmental variabilities recorded by pelagic sediments in the western Pacific during 15–11 Ma. *Palaeogeogr. Palaeoclimatol. Palaeoecol.* 628, 111776. doi: 10.1016/j.palaeo.2023.111776

Wang, F., He, G., Wang, H., and Ren, J. (2016). Geochemistry of rare Earth elements in a core from Mariana Trench and its significance. *Mar. Geol. Quat. Geol.* 36, 67–75. doi: 10.16562/j.cnki.0256-1492.2016.04.008

Wang, K., Shen, Y., Yang, Y., Gan, X., Liu, G., Hu, K., et al. (2019). Morphology and genome of a snailfish from the Mariana Trench provide insights into deep-sea adaptation. *Nat. Ecol. Evol.* 3, 823–833. doi: 10.1038/s41559-019-0864-8

Windom, H. L. (1969). Atmospheric dust records in permanent snowfields: implications to marine sedimentation. *Geol. Soc Am. Bull.* 80, 761–782. doi: 10.1130/0016-7606(1969)80[761:adrips]2.0.co;2

Xiao, C., Wang, Y., Tian, J., Wang, X., and Xin, Y. (2020). Mineral composition and geochemical characteristics of sinking particles in the Challenger Deep, Mariana Trench: Implications for provenance and sedimentary environment. *Deep-Sea. Res.* Pt I 157, 103211. doi: 10.1016/j.dsr.2019.103211

Xu, D., Yi, L., Yuan, H., and Chen, W. (2022). Geochronological evidence inferring carbonate compensation depth shoaling in the philippine sea after the mid-brunhes event. *J. Mar. Sci. Eng.* 10, 745. doi: 10.3390/jmse10060745

Yi, L. (2023). Diverse glacial ventilation in deep Pacific: An integrated record from Mariana Trench and Magellan Seamounts over last 1.2 Myr. *Glob. Planet. Change* 230, 104279. doi: 10.1016/j.gloplacha.2023.104279

Yi, L., Hu, B., Zhao, J., Jiang, X., Shu, Y., Wang, X., et al. (2022). Magnetostratigraphy of abyssal deposits in the central philippine sea and regional sedimentary dynamics during the quaternary. *Paleoceanogr. Paleoclimatol.* 37, e2021PA004365. doi: 10.1029/2021PA004365

Yi, L., Wang, H., Deng, X., Yuan, H., Xu, D., and Yao, H. (2021). Geochronology and geochemical properties of mid-pleistocene sediments on the caiwei guyot in the northwest pacific imply a surface-to-deep linkage. *J. Mar. Sci. Eng.* 9, 253. doi: 10.3390/jmse9030253

Yi, L., Xu, D., Jiang, X., Ma, X., Ge, Q., Deng, X., et al. (2020). Magnetostratigraphy and authigenic 10Be/9Be dating of plio-pleistocene abyssal surficial sediments on the southern slope of mariana trench and sedimentary processes during the mid-pleistocene transition. *J. Geophys. Res. Oceans.* 125, e2020JC016250. doi: 10.1029/2020JC016250

Yi, L., Yu, H.-J., Ortiz, J. D., Xu, X.-Y., Chen, S.-L., Ge, J.-Y., et al. (2012a). Late Quaternary linkage of sedimentary records to three astronomical rhythms and the Asian monsoon, inferred from a coastal borehole in the south Bohai Sea, China. *Palaeogeogr. Palaeoclimatol. Palaeoecol.* 329-330, 101–117. doi: 10.1016/j.palaeo.2012.02.020

Yi, L., Yu, H., Ortiz, J. D., Xu, X., Qiang, X., Huang, H., et al. (2012b). A reconstruction of late Pleistocene relative sea level in the south Bohai Sea, China, based on sediment grain-size analysis. *Sediment. Geol.* 281, 88–100. doi: 10.1016/j.sedgeo.2012.08.007

Zhang, W., De Vleeschouwer, D., Shen, J., Zhang, Z., and Zeng, L. (2018). Orbital time scale records of Asian eolian dust from the Sea of Japan since the early Pliocene. *Quat. Sci. Rev.* 187, 157–167. doi: 10.1016/j.quascirev.2018.03.004